Proceedings of the 16th International Heat Transfer Conference, IHTC-16
August 10-15, 2018, Beijing, China

IHTC16-24145

IMPROVING ELECTROLYTE TRANSPORT INSIDE THE LI-ION POROUS ELECTRODES USING MICROCHANNELS

Shahabeddin K. Mohammadian, Yuwen Zhang*

University of Missouri, Columbia, MO 65201, USA

ABSTRACT

Effects of using microchannels on the electrolyte transport inside the positive and negative electrodes have been investigated in this paper. A two-dimensional Lattice Boltzmann Method (LBM) simulation was carried out and a two-phase intermolecular potential model was utilized to investigate the microscopic behavior of the electrolyte flow in the porous electrodes. It was found that embedding microchannels inside the electrodes significantly improves the electrolyte transport inside both positive and negative electrodes. Furthermore, there is an optimum number of microchannels after which increasing the number of microchannels has no positive effect on the electrolyte transport inside the electrodes. Finally, the number of microchannels in the anode should be less than the number of the microchannels in the cathode in order to uniform electrolyte transport inside the both negative and positive electrodes.

KEYWORDS: Wettability, Mass Transfer, Electrolyte Transport, Li-ion batteries, Lattice Boltzmann method

1. INTRODUCTION

Electrolyte transport in a porous electrode is one of the most critical problems that is not well understood. The electrodes are generally a particle-based porous medium that allows the transport of electrons and ions through the particles and electrolytes in the void space [1]. Based on the United States Advanced Battery Consortium (USABC), the long-term goals for energy and power densities are 300 Wh/L and 600 W/L, respectively [2]. Achieving these goals requires to make high compressed electrodes. Increasing the electrodes compression decreases their porosity and increases the pore blockage. It also decreases the rate of the electrolyte transport inside the electrodes that causes lower wettability, which increases the electrical resistance inside the electrodes that leads to lower electrochemical performance of the battery cell. Therefore, electrolyte transport inside the electrodes and wettability are critical factors that should be considered in the process of designing new high-power demand Li-ion batteries.

Both positive and negative electrodes should be fully wetted with the electrolyte to maintain high utilization of electrode capacity. Insufficient wetting deteriorates the battery performance, and leads to decrease the safety of the battery due to extrusion of lithium metal. Furthermore, insufficient wetting accelerates the degradation of the Li-ion batteries that decreases the life of the battery. Thus, electrolyte transport inside the electrodes has been studied during the past decade. Wu et al. [3] investigated the wettability of both positive and negative electrodes and showed that electrolyte penetration and spreading in pores control the wettability of the porous electrodes, and wettability of the electrodes could be effected by organic solvent composition and lithium salt concentration. Stefan et al. [4] studied the effects of surface free energy and contact angle on various separators and electrodes. Yu et al. [5] showed that at the thick and dense electrodes, insufficient wetting degraded discharge capacity rapidly at high current rates. Chu et al. [6] investigated the influence of compaction on the porosity and electrochemical properties of a positive electrode and found wettability would be predominant at high C rates. Xie et al. [7] found that good wettability of the polyolefin separator had positive impacts on the lithium dendrite suppression and rate performance of lithium metal batteries.

*Corresponding Author: zhangyu@missouri.edu

Lattice Boltzmann Method (LBM) is an appropriate approach to simulate electrolyte transport in a porous electrode. It was first developed to simulate the phenomena, including fluid flow, heat transfer, and chemical reactions, at mesoscale. Theoretically, it is based on kinetic equations and statistical physics to simulate transport phenomena by tracking movements of molecule ensembles or the evolution of the distribution function [8]. This method can be used to simulate the complicated fluid flows such as chemically reacting, multiphase, and multicomponent flows. In LBM, fluid motion is simulated at the level of distribution functions. Therefore, the microscopic physics of the fluid particles could be incorporated as easily as in other particle collision methods. Besides, this approach has following attractive advantages: the high scalability in parallelism, simplicity in programming, ease in incorporating microscopic interactions, and simplicity in modelling complex geometry of flow problems [9]. Using LBM, electrolyte transport in the porous electrode was studied by Lee et al. [1] and it was shown that LBM could be effectively carried out to simulate liquid electrolyte behaviour in the porous electrodes. Paying attention to the compression ratio of the electrodes, Lee and Jeon [10] studied the wettability of the porous electrodes and found that increasing the compression ratio reduces the wettability. Recently, Mohammadian and Zhang [11] investigated the effects of microchannels on the wettability of the porous electrodes and showed that microchannels significantly increase the wettability, specifically electrodes with lower porosities.

In this study, liquid electrolyte transport in both positive and negative electrodes was investigated. A two-dimensional LBM approach was carried out and the two-phase intermolecular potential model [12, 13] was utilized to simulate the electrolyte flow in the electrodes. Since the two main challenges for the electrolyte transport in the Li-ion batteries are enhancing the wettability of the electrodes and improving the electrolyte filling time [1], the objective of this study is to investigate the effects of embedding some microscale grooves inside the electrodes as microchannels on both wettability and electrolyte filling time. Electrolyte transport inside the positive and negative electrodes is investigated. Since fewer number of the microchannels leads to lower pumping power need to flow the electrolyte inside the electrodes, the objective of this work is to find the optimum number of microchannels in both electrodes.

2. MODEL DESCRIPTION

LBM Model

LBM is a promising numerical approach that is very suitable for studying the fluid flow and diffusion through porous media that involves single or multiple components [14]. In this study, the LBM with the lattice Bhatnagar-Gross-Krook (BGK) model was carried out which the discrete particle distribution functions f_i are as follow:

$$f_i(x + e_i\Delta t, t + \Delta t) = f_i(x,t) - \frac{\Delta t}{\tau}\left[f_i(x,t) - f_i^{eq}(x,t)\right] + S_i(x,t) \quad (1)$$

where $f_i(x,t)$ is the probability of finding a particle in the ith velocity e_i at (x,t), Δt is the time step, and $S_i(x,t)$ is a source term. τ is the dimensionless relaxation time and is related to the kinetic viscosity v. f_i^{eq} is the equilibrium distribution and is given as follows:

$$f_i^{eq} = \rho w_i\left(1 + \frac{\vec{e_i}.\vec{u}^{eq}}{c_s^2} + \frac{(\vec{e_i}.\vec{u}^{eq})^2}{2c_s^4} + \frac{(\vec{u}^{eq})^2}{2c_s^2}\right) \quad (2)$$

where c_s is the speed of sound that defines as $c/3$, where $c = \Delta x/\Delta t$. w_i is the weight factor that for a two-dimensional nine velocities (D2Q9) model is define as:

$$w_i = \begin{cases} \frac{4}{9} & i = 1 \\ \frac{1}{9} & i = 2,3,4,5 \\ \frac{1}{36} & i = 6,7,8,9 \end{cases} \quad (3)$$

and $\vec{e_i}$ defines as

$$[e_1, e_2, e_3, e_4, e_5, e_6, e_7, e_8, e_9] = \begin{bmatrix} 0 & 1 & 0 & -1 & 0 & 1 & -1 & -1 & -1 \\ 0 & 0 & 1 & 0 & -1 & 1 & 1 & -1 & -1 \end{bmatrix} \quad (4)$$

Based on Shan-Chen pseudo-potential model, the density and equilibrium velocity of component γ were defined as:

$$\rho_\gamma = \sum_{i=1}^{9} f_{i,\gamma} \quad (5)$$

$$u_\gamma^{eq} = u' + \frac{\tau_\gamma F_\gamma}{\rho_\gamma} \tag{6}$$

where $u' = \sum_\gamma \rho_\gamma u_\gamma / \rho$, and F_γ is the Shan Chen force that is defined as [15].

$$F_\gamma(x) = -\psi_\gamma(x) \sum_{\tilde{\gamma} \neq \gamma} G_{\gamma\tilde{\gamma}} \sum_{i=1}^{9} w_i \psi_{\tilde{\gamma}}(x + e_i \Delta t) e_i \Delta t \tag{7}$$

where $\psi(\rho) = \rho_0[1 - exp(-\rho/\rho_0)]$, and $G_{\gamma\tilde{\gamma}}$ is a simple scalar that controls the strength of the interaction.

Reconstruction of porous electrodes

In order to generate electrodes with different porosities, a random porous medium generator code was employed. To represent the porous electrodes, a binary matrix in which "0" shows a fluid particle and "1" shows a solid particle has been utilized. To create porous electrodes, first the matrix was filled by ones (solid part), and next the program tunneled through the solid part by creating zeros (pores) at several fixed starting points and the process continued by creating more zeros around the previous pores until obtaining a desired porosity of the matrix. The positive electrode's porosity (cathode) is about 0.4, and the negative electrode's porosity (anode) is about 0.5-0.6 [16]. Therefore, in this study as illustrated in Fig. 1, a porous geometry with the porosities of 0.6 was built for negative electrode and a porous geometry with the porosity of 0.4 was created for positive electrode.

Numerical solution procedure

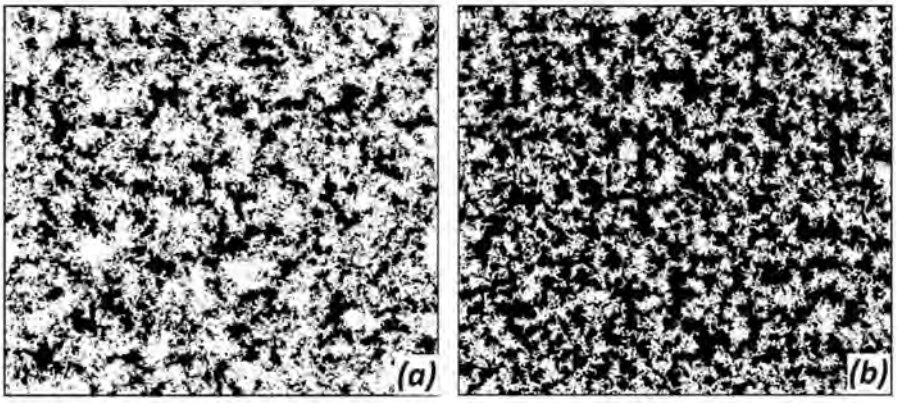

Fig. 1 Porous medium generation (a) Anode electrode p=0.6 (b) Cathode electrode p=0.4.

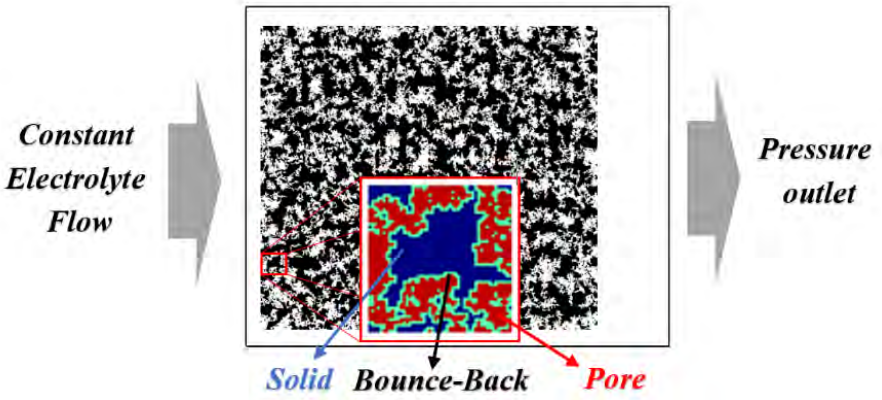

Fig. 2 Boundary Conditions.

In this study, Shan-Chen (SC) model was employed. This model is a bottom-up approach and is intrinsically simple. A bottom-up approach postulates a microscopic interaction between fluid elements that could be in the form of interaction potentials which leads to macroscopic separation of phases [15]. Two fluids consisted in this study are a gas (nitrogen or argon, blue in Figures 4 to 7) and liquid electrolyte (red in Figures 4 to 7) that penetrated in the porous electrodes. Figure 2 shows the two-dimensional domain size of 1000 × 800 lu² (lu: lattice unit, 1 lu means 1.25 μm of the physical length in this study) that was selected to simulate the electrolyte transport in both positive and negative electrodes. On the solid-liquid interface, bounce-back boundary condition was applied, and the inlet condition on the left was set with the flow velocity of 0.0083 lu and Reynolds number was 40. A fixed pressure condition was applied at the right.

In a two-phase flow in porous electrodes, capillary forces between the fluid-fluid and fluid-solid interfaces play dominant roles. The capillary number, which is the ratio of viscous to surface tension forces ($Ca = u\mu/\sigma$), for electrolyte flow is in the order of 10^{-5} [10] and in this study was 6.23×10^{-5}. Analyzing capillary and Reynolds numbers showed that the effects of viscosity and density ratios (that are about 100 and 1000, respectively) should be small and could be neglected [1]. Thus, the capillary force dominates the electrolyte flow, and viscous, buoyancy, and inertia forces were neglected.

The pressure inside a droplet is increased by the curved surface of the droplet in the mechanical equilibrium. For a 2D droplet, the pressure difference, the surface tension and the droplet radius have relationship that is known as the Young-Laplace Test [15]:

$$\Delta p = p_{in} - p_{out} = \frac{\sigma}{r} \tag{8}$$

where p_{in}, p_{out}, σ, and r are the inside and outside pressures of the droplet, the surface tension, and the radius of the droplet at the interface, respectively. As illustrated in Fig. 3, a computational domain of a droplet was employed in a 100 × 100 lu² to validate the present LBM. Increasing the inverse of the droplet radius leads to linear increase in the pressure difference which confirms that the utilized LBM can simulate the two-phase flow accurately.

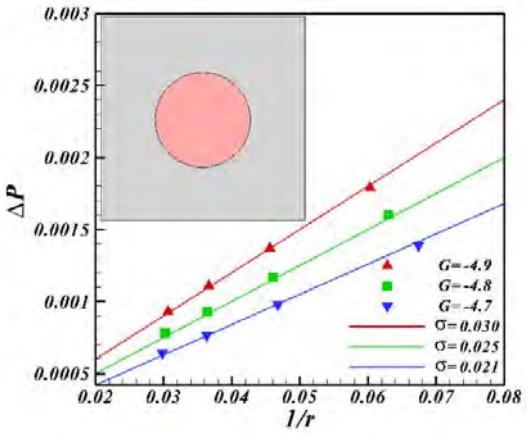

Fig. 3 Young-Laplace test validation.

3. RESULTS AND DESCUSSION

In this study one sixth of the porous electrodes has been utilized to embed microscale grooves as microchannels inside the electrodes. In order to compare the different numbers of microchannels, the total size of the microchannels considered to be the same (one sixth of the porous electrodes). It means with increasing the number of microchannels, their width decreases by the ratio of one over the number of microchannels. In other words. the width of the microchannel for the electrodes with one microchannel is $150\mu m$. The width of the microchannels for the electrodes with two, three, four, and five microchannels are $75\mu m, 50\mu m, 37.5\mu m,$ and $30\mu m$, respectively.

Figure 4 shows the electrolyte transport inside the anode (negative electrode) for the cases of without microchannels and with five microchannels in different timesteps. It can be seen that electrode with five microchannels is completely wetted after 200,000 timesteps. However, electrode without microchannels is still full of trapped gas. It clearly shows that microchannels have this ability to take the trapped gas inside the electrodes out of the battery and consequently improve the wettability of the electrodes.

Electrolyte transport through the pores of the negative electrode with the porosities of 0.6 after 200,000 timesteps has been illustrated in Fig. 5. It can be seen that electrolyte transport inside the anode porous electrode without any microchannels is too weak and after 200,000 time steps most of the electrode is still not wetted. For anode electrodes with one, two, and three microchannels, there are some spots that shows trapped gas could not be taken out. However, anode electrodes with four and five microchannels are almost free of trapped gas. It can be seen clearly that embedding microchannels inside the anode electrode improves the electrolyte transport and with increasing the number of microchannels this improvement enhances. However, comparing the electrodes with four and five microchannels shows that there is no significant difference between their wettability. It can be concluded that there is an optimum number of microchannels after which increasing the number of microchannels has no positive effect on the electrolyte transport inside the electrodes. Furthermore, it should be mentioned that fewer number of the microchannels leads to lower pumping power need to flow the electrolyte inside the electrodes.

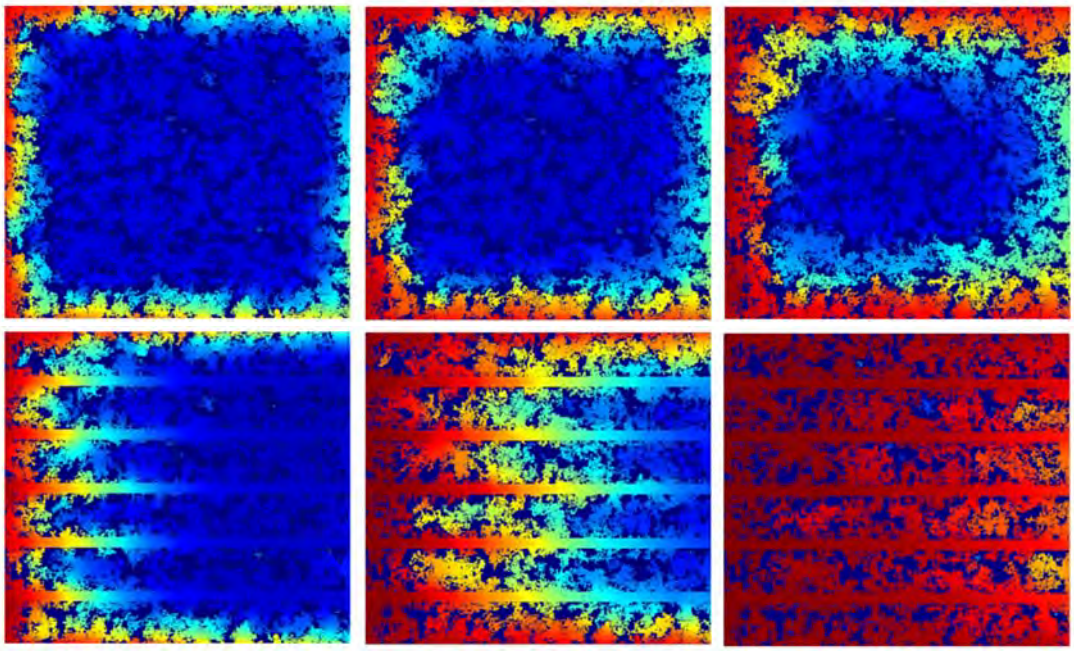

Fig. 4 Electrolyte transport in anode electrode after 50,000 timesteps (Left), 100,000 timesteps (middle), and 200,000 (right) timesteps.

Electrolyte transport through the pores of the positive electrode with the porosities of 0.4 after 500,000 timesteps has been illustrated in Fig. 6. It was found that cathode electrode with five microchannels became completely wet after 500,000 timesteps. Same as the results for anode electrodes, Fig. 6 shows that electrolyte transport inside the cathode porous electrode without any microchannels is too weak and after 500,000 timesteps most of the electrode is still not wetted. Also, embedding microchannels inside the cathode electrode can significantly improve the electrolyte transport. Again, results for cathode electrodes with four and five microchannels are almost the same. However, paying more attention to the results, it can be found that the number of blocked area where the gas trapped there (light blue spots) is fewer for cathode electrode with five microchannels.

It was found from the above results that cathode electrode with the porosity of 0.4 and five microchannels (best option) needs 500,000 timesteps to become completely wet. However, anode electrode with higher porosity

(p=0.6) needs fewer timesteps to be completely wetted. Or, for a same timesteps, it needs fewer number of microchannels. As illustrated in Fig. 7, after 500,000 timesteps anode electrodes with two or more microchannels are completely wetted. It means that two microchannels in enough for anode. Therefore, the number of microchannels in the anode (negative electrode) should be fewer than the number of the microchannels in the cathode (positive electrode) due to uniform electrolyte transport inside the both positive and negative electrodes. Embedding fewer number of the microchannels inside the anode decreases the pumping power required for electrolyte flow.

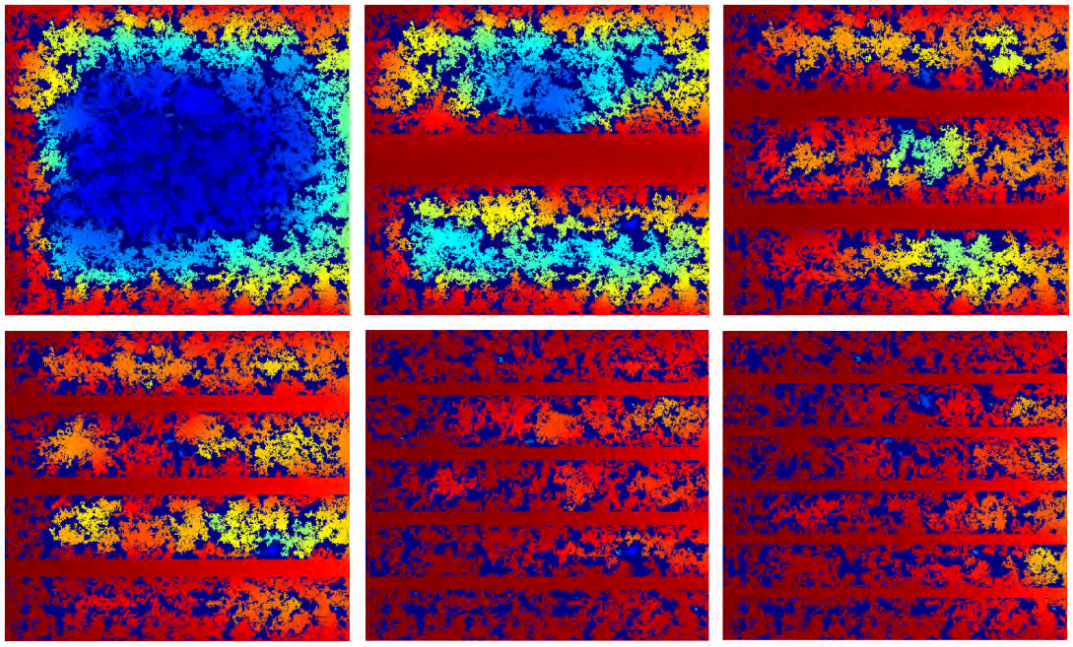

Fig. 5 Electrolyte transport in anode electrode after 200,000 timesteps.

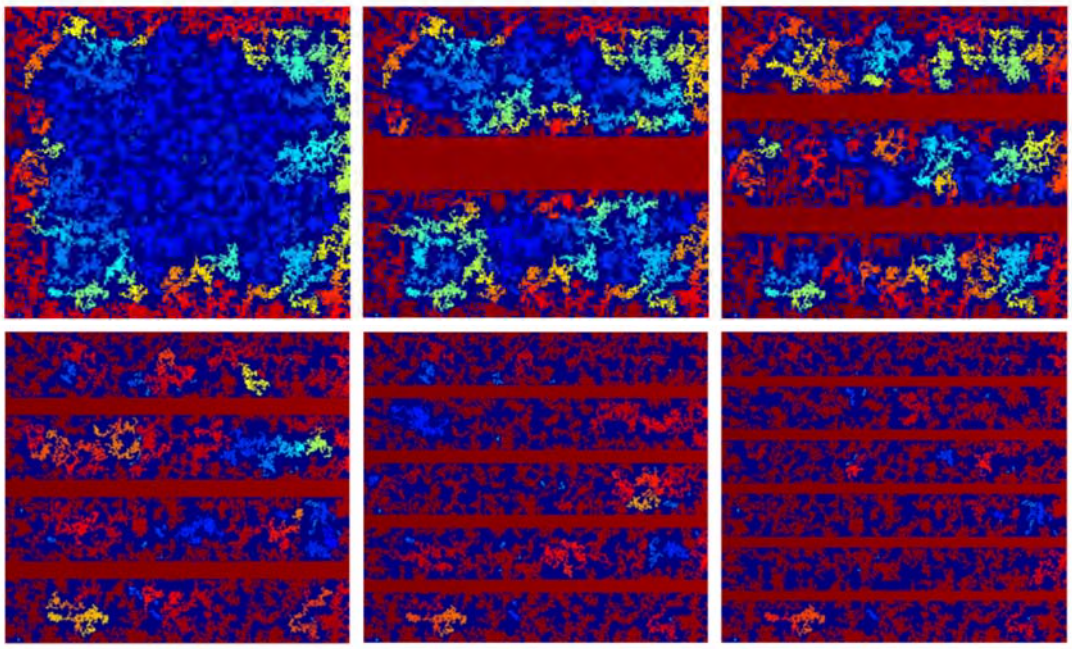

Fig. 6 Electrolyte transport in cathode electrode after 500,000 timesteps.

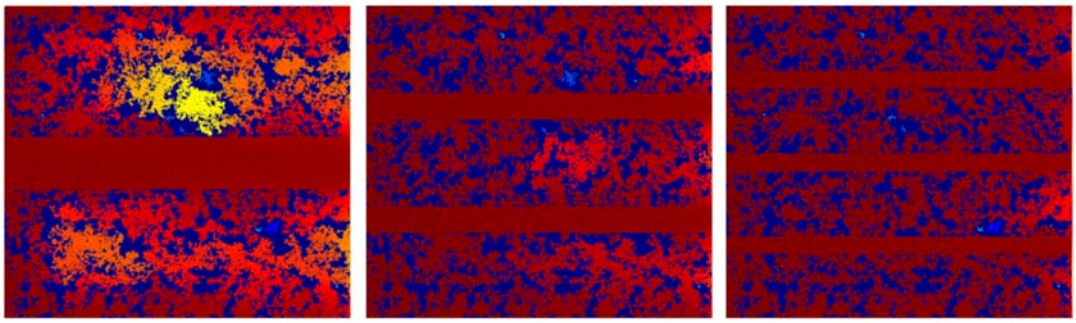

Fig. 7 Electrolyte transport in anode electrode after 500,000 timesteps.

4. CONCLUSIONS

In this study, the effects of embedded microchannels on the electrolyte transport inside both positive and negative electrodes was studied. Two-dimensional LBM simulation was carried out to simulate the effects of embedded microchannels inside the electrodes on the electrolyte transport. The results showed that:

- Embedding microchannels inside the electrodes significantly improves the electrolyte transport inside both positive and negative electrodes.
- There is an optimum number of microchannels after which increasing the number of microchannels has no positive effect on the electrolyte transport inside the electrodes.
- The number of microchannels in the anode (negative electrode) should be less than the number of the microchannels in the cathode (positive electrode) due to uniform electrolyte transport inside the both positive and negative electrodes. For the size and porosity assumptions of this study, for each five microchannels in the cathode, only two microchannels is required for anode.

NOMENCLATURE

Ca	Capillary number	
c_s	speed of sound	(m/s)
e_i	lattice velocity	(m/s)
f	distribution function	
F_γ	Shan Chen force	
G	Green's function (simple scalar)	
p	pressure	(pas)
Δp	pressure difference	(pas)
r	radius of the droplet	(m)
Re	Reynolds number	
S	source term	
u	velocity	(m/s)
w	weight coefficient	
Greek		
ρ	density	(kg/m^3)
υ	kinetic viscosity	(m^2/s)
σ	surface tension	(N/m)
ψ	function of density	
τ	relaxation time	
μ	dynamic viscosity	(kg/m s)
Subscript		
eq	equilibrium	
γ	component	
in	inside	
out	outside	

REFERENCES

[1] S.G. Lee, D.H. Jeon, B.M. Kim, J.H. Kang, C.-J. Kim, Lattice Boltzmann Simulation for Electrolyte Transport in Porous Electrode of Lithium Ion Batteries, Journal of The Electrochemical Society, 160 (2013) H258-H265.

[2] N.R. Council, Effectiveness of the United States Advanced Battery Consortium as a Government-Industry Partnership, The National Academies Press, Washington, DC, 1998.

[3] M.-S. Wu, T.-L. Liao, Y.-Y. Wang, C.-C. Wan, Assessment of the Wettability of Porous Electrodes for Lithium-Ion Batteries, Journal of Applied Electrochemistry, 34 (2004) 797-805.

[4] C.S. Stefan, D. Lemordant, B. Claude-Montigny, D. Violleau, Are ionic liquids based on pyrrolidinium imide able to wet separators and electrodes used for Li-ion batteries?, Journal of Power Sources, 189 (2009) 1174-1178.

[5] S. Yu, Y. Chung, M.S. Song, J.H. Nam, W.I. Cho, Investigation of design parameter effects on high current performance of lithium-ion cells with LiFePO4/graphite electrodes, Journal of Applied Electrochemistry, 42 (2012) 443-453.

[6] C.-M. Chu, C.-Y. Liu, Y.-Y. Wang, C.-C. Wan, C.-R. Yang, On the evaluation of the factors influencing the rate capability of a $LiCoO_2$|Li battery, Journal of the Taiwan Institute of Chemical Engineers, 43 (2012) 201-206.

[7] Y. Xie, H. Xiang, P. Shi, J. Guo, H. Wang, Enhanced separator wettability by LiTFSI and its application for lithium metal batteries, Journal of Membrane Science, 524 (2017) 315-320.

[8] X. He, N. Li, Lattice Boltzmann simulation of electrochemical systems, Computer Physics Communications, 129 (2000) 158-166.

[9] Q. Liao, T. Chein Jen, Application of Lattice Boltzmann Method in Fluid Flow and Heat Transfer, Chapter 2, in: Computational Fluid Dynamics Technologies and Applications, 2011.

[10] S.G. Lee, D.H. Jeon, Effect of electrode compression on the wettability of lithium-ion batteries, Journal of Power Sources, 265 (2014) 363-369.

[11] S.K. Mohammadian, Y. Zhang, Improving wettability and preventing Li-ion batteries from thermal runaway using microchannels, International Journal of Heat and Mass Transfer, 118 (2018) 911-918.

[12] X. Shan, H. Chen, Lattice Boltzmann model for simulating flows with multiple phases and components, Physical Review E, 47 (1993) 1815-1819.

[13] X. Shan, H. Chen, Simulation of nonideal gases and liquid-gas phase transitions by the lattice Boltzmann equation, Physical Review E, 49 (1994) 2941-2948.

[14] K.S.W. Chiu, S.A. Joshi, N.K. Grew, Lattice Boltzmann model for multi-component mass transfer in a solid oxide fuel cell anode with heterogeneous internal reformation and electrochemistry, The European Physical Journal Special Topics, 171 (2009) 159-165.

[15] T. Krüger, H. Kusumaatmaja, A. Kuzmin, O. Shardt, G. Silva, E.M. Viggen, The Lattice Boltzmann Method Principles and Practice, (2017).

[16] M. Singh, J. Kaiser, H. Hahn, Effect of Porosity on the Thick Electrodes for High Energy Density Lithium Ion Batteries for Stationary Applications, Batteries, 2 (2016).